Wall shear stress and mass transfer rates – important parameters in CO_2 corrosion

M LANGSHOLT, M NORDSVEEN, and **K LUNDE**
Institute for Energy Technology, Kjeller, Norway
S NESIC
Department of Mechanical Engineering, The University of Queensland, Australia
J ENERHAUG
Statoil Research Centre, Trondheim, Norway

ABSTRACT

The modelling and understanding of fluid flow and CO_2-corrosion is of decisive importance for economic and safe use of multiphase transport technology. Shear stresses and shear stress fluctuations at the wall can have a significant effect on the survival of the corrosion product films and the inhibitor persistency. In addition, the shear stress is important for the liquid holdup and the pressure drop through the pipeline. Mass transfer rates of species towards and from the pipe wall is one of the parameters which influence the CO_2-corrosion rates.

This paper presents the results from a study of stratified two-phase flow in a horizontal pipe, focusing on the measurement of wall shear stresses and mass transfer rates. In addition, standard parameters such as superficial velocities, pressure drop and liquid holdup in the test section were measured. Two different techniques were used to measure the wall shear stresses. These are the hot-film technique and an electrochemical method - which compared well. The latter method was also used for the measurement of the mass transfer rates.

The mean hydrodynamic flow data prove to agree well with predictions obtained with the steady state two-phase flow model WOLGAS95. However, the modelling of mean mass transfer rates based on this flow model and the Berger & Hau (1977) correlation is shown not to compare favourably with the presented experimental data.

---

[1] **Present address: Department of Mechanical Engineering, The University of Queensland, Brisbane Qld 4072, Australia.**

NOMENCLATURE

A	cross sectional area of pipe	[m^2]
A'	hot-film calibration constant	[-]
B'	hot-film calibration constant	[-]
c_{O_2}	concentration of oxygen in the water	[ppm]
D	diffusion coefficient (=1.93 for oxygen)	[m^2/s]
d	pipe diameter	[m]
E_{Bridge}	Hot-film anemometer bridge voltage	[V]
dP/dx	frictional pressure gradient along pipe	[Pa/m]
F	Faraday constant (=96490)	[*C/equiv*]
g	acceleration due to gravity (=9.81)	[m/s^2]
H	liquid holdup	[-]
i_{lim}	limiting current	[A]
k_m	mass transfer coefficient	[cm/s]
l	streamwise length of electrode	[m]
Re	Reynolds number (= Ud/ ν)	[-]
S	length of interface, including wetted perimeter	[m]
Sc	Schmidt number (= ν/D)	[-]
Sh	Sherwood number (= k_m d/D)	[-]
U	velocity	[m/s]

Greek symbols

α	gas void fraction	[-]
β	pipe inclination	[deg]
μ	dynamic viscosity	[kg/ms]
ν	kinematic viscosity	[m^2/s]
ρ	phase density	[kg/m^3]
τ	shear stress	[Pa]

Subscripts

i	interface
l	liquid phase
g	gas phase
s	superficial, as in superficial velocities
w	wall

1. INTRODUCTION

Corrosion can be affected by flow differently depending on the mechanism governing the corrosion process. One can arbitrarily discriminate two major cases:

- effect of flow on corrosion when no surface films are present and
- effect of flow on corrosion in the presence of surface films (precipitates, inhibitors, etc.)

In the no-film case the primary effect of flow on corrosion is through the mass transfer of the species involved in the corrosion reaction at the metal surface. When surface films are present they can reduce the corrosion rate by preventing the transport of species involved in the electrochemical reactions at the metal surface. The results presented here are obtained for film-free surfaces. A follow-up study focusing on possible flow induced inhibitor film removal has recently been started.

The exploitation of major gas-condensate fields on the Norwegian continental shelf, exemplified by the Åsgard and Troll fields, have over the past years initiated extensive research related specifically to problems encountered in gas-condensate transport systems. The present work falls into this category, with highlight on the stratified gas-liquid flow regime in a horizontal pipe - a typical situation for a gas condensate pipeline.

2. EXPERIMENTAL FACILITY AND INSTRUMENTATION

2.1 The flow loop

The experimental lab facility used for this study was Institute for Energy Technology's (IFE's), permanent, medium pressure, multi-phase flow loop. It is a closed system utilising the dense gas sulphur hexafluorid, SF_6, which at the maximum operating pressure of 10 bar has a density of 60 kg/m^3. The main benefit of using a dense gas is that we, at a moderate loop pressure, achieve the high gas-to-liquid density ratio found in real, high pressure, petroleum pipelines. The facility is fully equipped to handle three-phase flow (water/oil/gas). The general specifications for the loop are summarised in Table 1.

Maximum pressure	10 bar
Test section diameter	0.1 m
Test section length	15 m
Inclination of test section	0 - 90°
Superficial gas velocity range	0.3 - 12 m/s
Superficial liquid velocity range	0.02 - 3 m/s

Table 1. IFE's multiphase flow loop - general specifications.

The lab facility consists of four basic systems: fluids feeding, the test section, a system for fluids return and separation and a calibration section. A flow diagram of the loop is shown in Figure 2.

The test section and related instruments are shown in Figure 1. The total straight length of the test section is 15 m, with an internal diameter of 0.1 m. Of these 15 m the last 10 m are made from transparent PVC, enabling visual observation of the flow. The standard instrumentation consisted of a gamma densitometer for measurement of phase fractions (holdup), dp-cells for pressure drop measurements and an optical section for use with video or high speed film techniques. The gamma densitometer is based on a principle where the entire cross section is exposed to radiation, and thus measures the average liquid holdup independently of the phase distribution and with extremely short response times. More details are given by Nydal (1991).

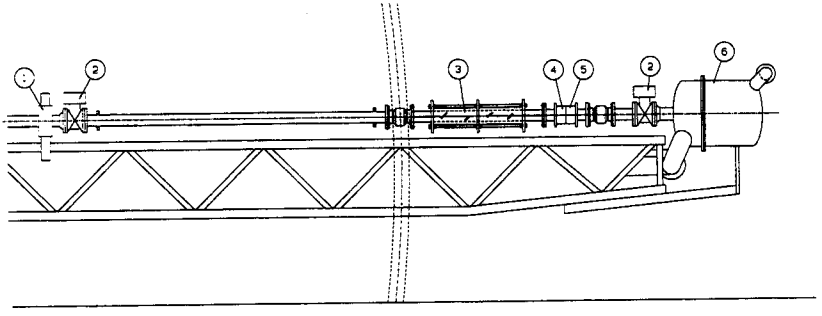

Figure 1. Outline of the test section part of the loop.(1): γ-densitometer, (2):Fast closing valves, (3): Optical section, (4): Hot-film probe, (5): Mass transfer probe, (6): End separator

2.2 The hot-film method

To measure the wall shear stress the hot film anemometry technique proposed by Shiralkar (1970) was adopted, using a flush mounted probe of the type Dantec 55R46 with 2 μm quartz coating. The probe was operated by a linearised, constant temperature anemometry system.

The hot-film probe was mounted in a specially designed plug, see Figure 3, which could easily be transferred between the test section and the calibration rig. The plug was then mounted flush with the pipe wall. The sensor is a thin film resistance element which is heated and controlled at an elevated temperature through the anemometer circuit. The amount of electrical energy dissipated in the sensor is a measure of the cooling effect of

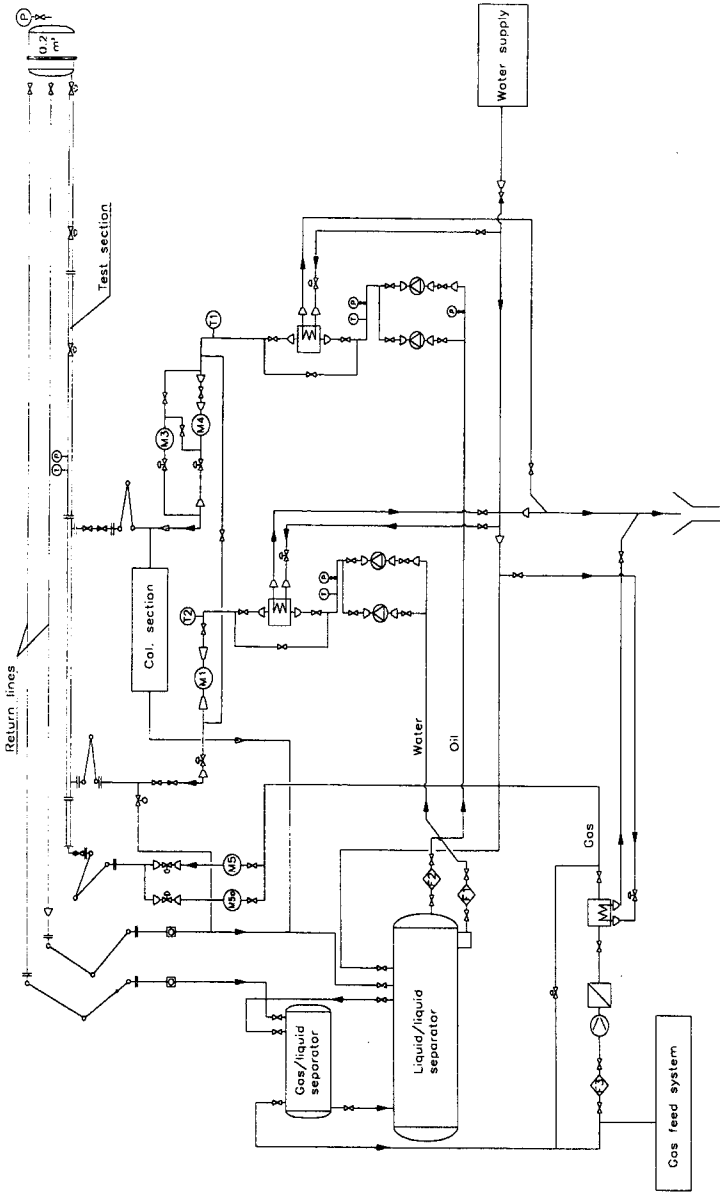

Figure 2. Flow diagram of the loop

the fluid flowing past the heated sensor. The size of the sensor element is 0.2 x 0.7 mm, and it was operated so that its longer side was perpendicular to the principal direction of flow, as indicated in Figure 3.

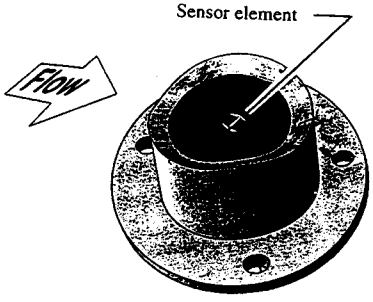

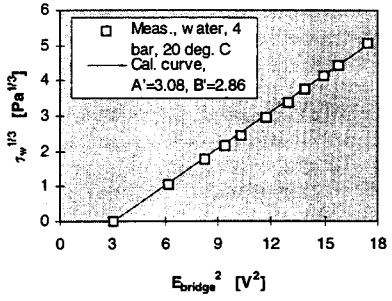

Figure 3. Hot-film probe mounted in plug *Figure 4. Typical hot-film calibration curve*

By considering the boundary layer problem associated with flow over a heated wall, it can be shown, see e.g. Bellhouse & Schultz (1966) or Spence and Brown (1967), that the bridge voltage, E_{Bridge}, of the anemometer is related to the wall shear stress, τ_w, as:

$$E_{Bridge}^2 = A' + B' \tau_w^{\frac{1}{3}} \quad (1)$$

In practice the calibration constants A' and B' are very sensitive to changes in ambient temperature, to contamination of the probe and to other factors which might result in a shift in the bridge voltage. Special care was taken to check and, if necessary, re-calibrate the probe. The probe was calibrated in a special rig at shear stresses up to 150 Pa and in addition frequently checked in situ by measuring the pressure drop in single phase flow of liquid. A typical calibration is plotted as $\tau_w^{1/3}$ *vs.* E^2 in Figure 4, and shows the expected linear trend.

2.3 The mass transfer probe - operating principle, design and procedure

In order to measure the mass transfer rates the electrochemical limiting diffusion current technique was used. It is a versatile and accurate technique for the investigation of the mass transfer and related hydrodynamic phenomena. The essence of this technique is that by polarising the working electrode one accelerates the electrochemical processes until the transport of the involved species to the metal surface becomes rate limiting. The transport process depends primarily on the diffusion through the boundary layer - which in turn is a function of the flow parameters. When the working electrode is polarised

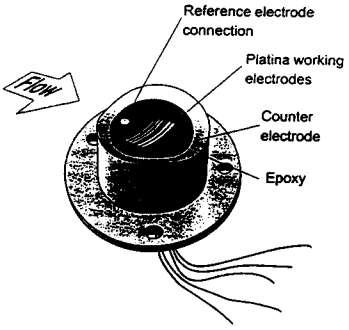

Figure 5. The mass transfer probe

properly then the measured limiting current is directly proportional to the mass transfer rate.

A probe for the measurement of the mass transfer rates was designed particularly for this study. In principle the probe consisted of: platinum working electrodes embedded into epoxy; a counter electrode - we found that using the body of the loop was the best solution; and an Ag/AgCl reference electrode. The reference electrode was connected to the loop via a salt bridge and a porous wooden plug. The probe actually included five rectangular platinum strips with the same width (20 *mm*) and different streamwise lengths (0.25, 0.5, 1.0 and 2.0 *mm*) - all mounted flush with the pipe wall, see Figure 5.

Due to the short streamwise length of the working electrode, a fully developed boundary layer was not present. The results, therefore, had to be converted into fully developed boundary layer conditions, present in steel pipelines, using theoretical considerations. On the other hand, using short electrodes had an advantage for our measurements. Since we were trying to measure fluctuations in the mass transfer rate found in multi-phase flow, long electrodes would have been sluggish in response and would lead to the averaging of the measured current over a large area. In both cases the high local mass transfer peaks which were expected in multi-phase flow would be "smeared out" or would pass unrecorded.

The contribution of the migration transport mechanism (ionic movement of species due to an electrical potential gradient) and the IR (Ohmic) drop were eliminated by adding 1% Na_2SO_4 to the water phase which increased the conductivity significantly. Oxygen was used as the active species for a few practical reasons. Firstly, it was possible to accurately monitor the oxygen concentration (10 *ppm* in our experiments) in the loop. Secondly, it is known that during reduction of oxygen it is possible to obtain clear and measurable limiting currents. In the two-phase flow tests only the 0.5 *mm* working electrode was used. All measurements were conducted using a potentiostat (with a floating option) connected with a PC.

In the loop, measurements were made initially in single-phase water flow. Potentio-dynamic sweeps were performed in order to identify the limiting current region. Subsequently potentiostatic measurements were conducted where the working electrode potential was held in the middle of limiting current range while the water flow rate was varied. Once the results were analysed and successfully compared with theory the same potentiostatic technique was used in multiphase flow. At the end, the probe was again tested in single-phase flow in order to determine if there had been any drift.

The measured limiting currents, i_{lim} , in single-phase flow were converted into the mass transfer coefficient, k_m , by using:

$$k_m = \frac{i_{\lim}}{4F \cdot c_{O_2}} \tag{2}$$

The results of these measurements in single-phase pipe flow are shown in Figure 6 for three of the working electrodes (l = 0.5, 1 and 2 *mm*). The mass transfer coefficient, k_m , is expressed in terms of a ratio of the Sherwood number $Sh = k_m\, d/D$ and the Schmidt number $Sc = \nu/D$, raised to the 0.33 power, so that the results are not dependent on the properties of the solution or the species involved. In addition this ratio was multiplied by the $(l/d)^{0.33}$ factor in order to eliminate the effect of different electrode lengths and partially developed boundary layers For short electrodes we have the theoretical based Shaw et al. correlation

$$Sh' = 0.276 \cdot Re^{0.58} \cdot Sc^{0.33} \left(\frac{l}{d}\right)^{-0.33} \tag{3}$$

All three curves are close to this correlation proving that the calibration measurements were successful.

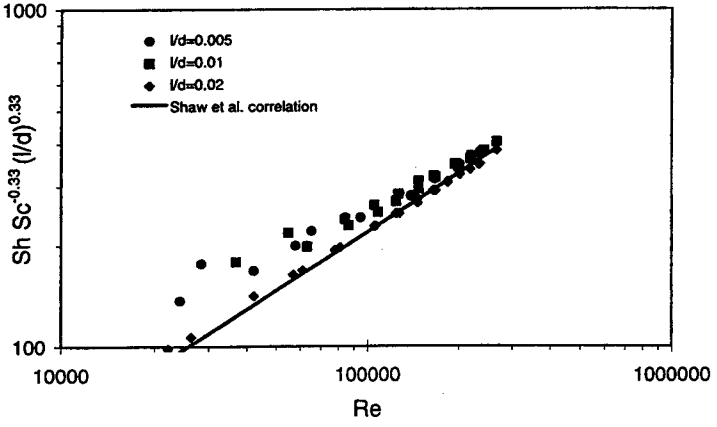

Figure 6. *Mass transfer measurements in single-phase water flow using three different working electrodes plotted with the correction for electrode length.*

A practical question now arises: how does one convert the mass transfer measurements obtained with short electrodes into mass transfer measurements which would have been obtained for fully developed boundary layer pipe flow? A mass transfer correlation for fully developed single-phase pipe flow is well established in the literature, Berger & Hau (1977):

$$Sh = 0.0165 \cdot Re^{0.86} \cdot Sc^{0.33} \tag{4}$$

Now, by eliminating the *Re*-number between Eqs. (3) and (4) we obtain:

$$Sh = 0.111 \cdot Sh'^{1.48} \cdot Sc^{-0.16} \left(\frac{l}{d}\right)^{0.49} \tag{5}$$

Since the mass transfer on short electrodes, *Sh'*, was measured in the two-phase flow experiments, eq. (5) was subsequently used to obtain the Sherwood numbers presented below. From the analogy of mass and momentum transfer and the fact that for large Schmidt numbers the mass transfer boundary layer is embedded in the viscous sublayer it can be shown, Nakoryakov et al. (1983), that the wall shear stress τ and the Sherwood number are related:

$$\tau = \frac{1.9 \mu D}{l^2} Sh^3 \tag{6}$$

Thus by conducting the mass transfer measurements one can convert the Sherwood number into the wall shear stress in a similar way as for the hot film probe. A calibration curve for the shear stress relation was established and used in the two-phase flow experiments.

3. EXPERIMENTAL PROCEDURES

All the reported experiments were made with a horizontal test section and with the fluids held at a temperature of 20°C. The liquid phase, water + 1% Na_2SO_4, and the gas phase had densities of 1006 kg/m^3 and 18.6 kg/m^3, respectively. Both the hot-film probe and the mass transfer probe were positioned at the bottom of the pipe. The logging frequency was 330 Hz for the hot-film probe and 100 Hz for the γ-densitometer and the mass transfer probe. A 5 Hz logger was set up for the temperature, the superficial velocities, the absolute loop pressure and the differential pressure over the dp-sections.

The operation of the loop and the measurements were carried out using the following stepwise procedure:

- The γ-densitometer was calibrated at least once a day
- The dP-cells were continuously monitored for shift or zero drift
- The oxygen content in the loop was kept at a constant 10 ppm level
- Hot-film and mass transfer probes were checked and/or calibrated
- Compressors and pumps were started and valves were adjusted so that desired flow rates were obtained
- Data acquisition from the various sensors was synchronised to within 1 second. The logging period for each experimental data point was typically 30 seconds.

4. EXPERIMENTAL RESULTS

The flow rates covered two 'levels' of superficial liquid velocities, 0.02 and 0.25 m/s, combined with superficial gas velocities in the range 1 to 8 m/s. The main descriptive statistics for each experiment are summarised in Table 2 below. In all cases a stratified wavy flow regime was obtained, with moderate amounts of gas being transported as bubbles in the liquid layer at the bottom of the pipe, see Lunde (1997).

Exp	U_{sg}	U_{sl}	dP/dx	H	U_g	U_l	τ_w (mass transfer probe)				τ_w (hot-film probe)				mass transfer $ShSc^{-0.33}$			
no							mean	stand.	max.	min.	mean	stand.	max.	min.	mean	stand.	max.	min.
							value	dev.	value	value	value	dev.	value	value	value	dev.	value	value
	m/s	m/s	Pa/m	%	m/s	m/s	Pa	Pa	Pa	Pa	Pa	Pa	Pa	Pa	[-]	[-]	[-]	[-]
1	2.14	0.021	16	6.1	2.28	0.34	0.9	0.2	1.5	0.5	0.2	0.1	0.8	0	191	13	236	153
2	4.11	0.019	53	2.0	4.19	0.95	4.7	0.2	5.3	4.2	2.8	1.3	8.7	0.7	370	7	388	352
3	6.34	0.025	115	1.2	6.42	2.08	7.6	0.3	8.4	7	5.9	2.4	16	1.1	448	6	466	433
4	6.06	0.25	188	11.1	6.82	2.25	11	0.7	13	9.5	13	3.9	28	2.6	523	12	557	489
5	7.1	0.25	242	9.5	7.85	2.63	14	0.7	17	12	15	4.1	32	3.4	571	12	612	542
6	8.18	0.25	313	8.2	8.91	3.05	16	0.8	19	14	18	4.4	38	4.8	611	12	651	578
7	5.05	0.25	146	12.9	5.8	1.94	11	0.9	13	8.9	11	3.5	22	2.2	520	16	564	478
8	4.1	0.25	112	15.4	4.84	1.62	9.3	0.6	11	7.2	8.6	2.6	16	1.3	486	13	527	439
9	3	0.25	74	19.4	3.72	1.29	6.4	0.6	8.2	4.9					419	17	463	375
10	2.03	0.25	41	27.2	2.79	0.92	3.6	0.3	4.6	2.7	2.6	0.9	6.8	0.7	332	11	367	298
11	0.96	0.25	28	42.0	1.66	0.6	2	0.7	5.3	1.1					261	34	384	205

Table 2. Summary of the results for the performed set of experiments (for symbols, see the nomenclature list).

The measured values of the mass transfer coefficient are shown in Figure 7 as a function of the water velocity (as calculated from the measured holdup). Since a power law relationship is obtained in single-phase flow, see eq. (8), it gives confidence to see that a straight line is obtained in a log-log plot. The maximum value of measured mass transfer was typically 10-30% higher than the mean value in this stratified wavy flow regime.

Figure 8 shows the wall shear stress plotted vs. the measured pressure drop. As can be seen the agreement of the mean wall shear stress measurements obtained with the two probes was good.

When it comes to the shear stress fluctuations it is clear that higher values were recorded with the hot film probe, see Figure 9 and Figure 10. The reason is that the logging frequency of the hot film probe was more than three times that of the mass transfer probe, so that any short lasting peaks were easier to "catch". In addition, due to the much smaller active area of the hot film probe its response time to changes in the flow was much shorter than that of the mass transfer probe. Thus the fluctuation measurements obtained with the hot film probe are probably more accurate.

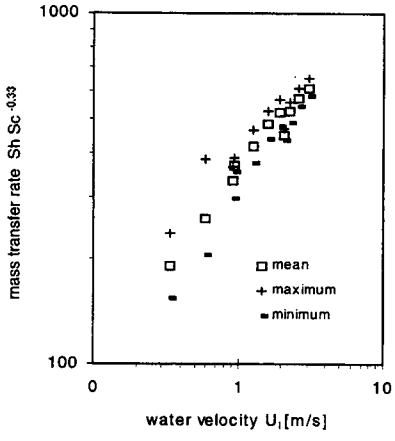

Figure 7. The mass transfer coefficient vs. the water velocity (as calculated from the holdup).

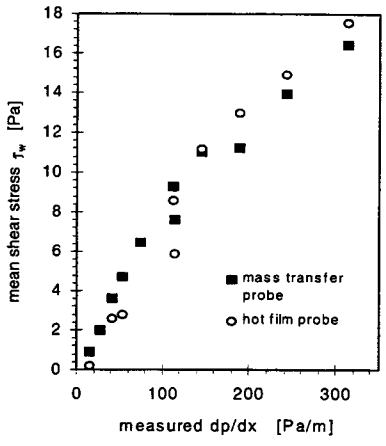

Figure 8. The wall shear stress vs. the pressure drop for the two different probes.

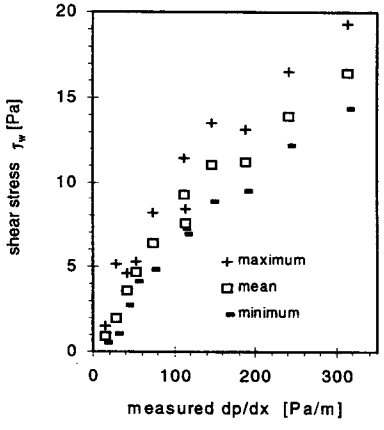

Figure 9. The wall shear stress vs. the pressure drop - mass transfer probe

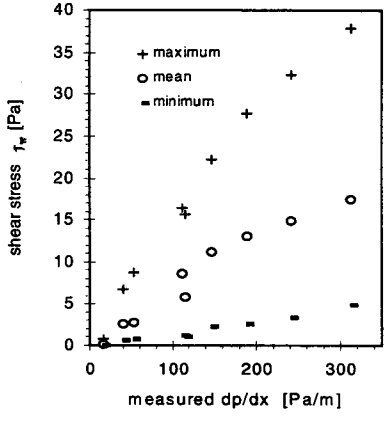

Figure 10. The wall shear stress vs. the pressure drop - hot-film probe

5. THEORETICAL BASIS - STRATIFIED TWO-PHASE FLOW MODEL

By considering the momentum balances for equilibrium stratified flow, see Figure 11, we arrive at the following set of equations:

$$\text{For the liquid phase : } -(1-\alpha)A(\rho_l g \sin\beta + \frac{dP}{dx}) - \tau_{wl} S_l + \tau_i S_i = 0 \tag{7}$$

$$\text{For the gas phase: } -\alpha A(\rho_g g \sin\beta + \frac{dP}{dx}) - \tau_{wg} S_g - \tau_i S_i = 0 \tag{8}$$

From the above equations together with closure laws for interfacial and wall shear stresses it is possible to develop a closed equation system which calculates the pressure drop and holdup/void given superficial velocities, densities, surface tension, pipeline inclination and cross section area. In a more complex situation there will be bubbles in the liquid phase and droplets in the gas phase, the flow may form other flow patterns and an additional water phase may be present as well. To simulate such complex cases a model named WOLGAS95 was developed at IFE. This model has been used for the predictions in this work.

By eliminating the pressure drop from Eqs. (7) and (8), we find for the interfacial shear stress

$$\tau_i = \tau_{wl}\frac{S_l}{S_i}\alpha - \tau_{wg}\frac{S_g}{S_i}(1-\alpha) + H\alpha g \sin\beta \frac{A}{S_i}(\rho_l - \rho_g) \tag{9}$$

Further, by eliminating the interfacial shear stress from Eqs. (7) and (8), we obtain an expression for the mean wall shear stress based on the measurement of pressure gradient and holdup:

$$-A\frac{dP}{dx} - HA\rho_l g \sin\beta - \alpha A \rho_g g \sin\beta = \tau_l S_l + \tau_g S_g = \bar{\tau}\pi D \tag{10}$$

The single-phase wall shear stress is calculated from the standard text book relation:

$$\tau_w = \frac{d}{4}\frac{dP}{dx} \tag{11}$$

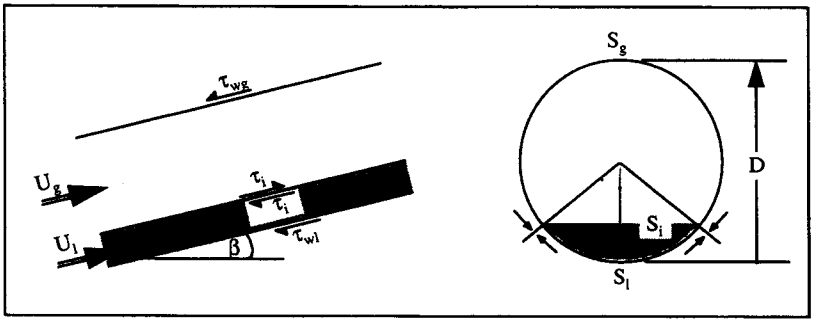

Figure 11. Stratified flow configuration in an inclined pipe

6. COMPARISON BETWEEN MEASUREMENTS AND PREDICTIONS

The experimental two-phase flow results have been compared with predictions based on WOLGAS95[1] (see above) and the Berger & Hau (1977) correlation for mass transfer correlations. Gas bubbles in the liquid layer is an optional parameter in WOLGAS95, consequently being activated in these tests. The density used for the film Reynolds number is then the mixture gas/liquid density. This Reynolds number enters the correlations for shear stresses, etc. This option had to be activated to obtain good predictions of the hydrodynamic parameters.

In Figure 12 and Figure 13 predicted hold-up and pressure drop are shown to agree reasonably well with the measurements, although an over-prediction of the pressure drop is observed for the higher gas velocities. Figure 14 shows that the predicted mean liquid-to-wall shear stress compares well with the measured mean value in the bottom of the pipe. However, it is known, Kowalski (1987), that the shear stress may vary a lot around the pipe perimeter. This effect has not been taken into account in the model.

The mass transfer rates predictions based on WOLGAS95, with gas in the liquid layer, and the Berger & Hau (1977) correlation, gave major discrepancies relative to the measured values, as can be seen in Figure 15. We used the gas/liquid mixture density also for the Reynolds number entering the Berger & Hau correlation. Improved modelling of mass transfer rates in multiphase flow seems to be necessary. In the literature the effects of bubbles on mass transfer rates have been reported, Economou & Alkire (1985), and an improved modelling of these effects could turn out to be important. Another possibly important effect, which is not taken into account in the present mass transfer calculations, is the influence of waves on the gas/liquid interface.

7. CONCLUSIONS

A series of two-phase flow experiments on stratified flow in a horizontal pipe has been performed in IFE's medium pressure multiphase flow loop. The main conclusions from the study can be summarised as follows:

- The liquid-to-wall shear stresses and mass transfer rates have been successfully measured. An electrochemical technique was used for the mass transfer measurements, from which also the wall shear stresses could be derived. Shear stresses measured with the mass transfer probe compared very well with the results from the hot-film probe, thus lending confidence to these results.

- At the bottom of the pipe the maximum value of the shear stress was typically 2 - 4 times the mean value. The maximum value of measured mass transfer in the stratified-wavy flow regime was typically 10-30% higher than the mean value, also measured at the bottom of the pipe.

---

[1] WOLGAS95 is IFE's 'in-house' steady state two/three-phase flow point model

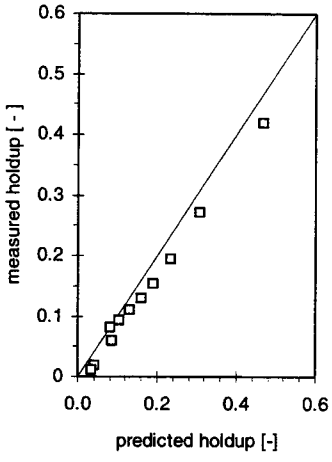

Figure 12. Comparison between measured and WOLGAS95 predicted holdup

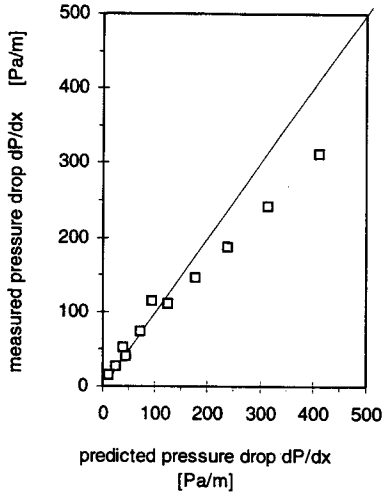

Figure 13. Comparison between measured and WOLGAS95 predicted pressure drop

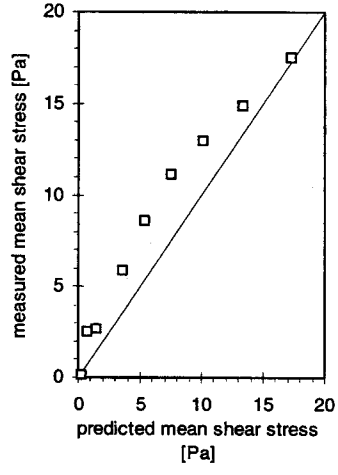

Figure 14. Comparison between measured and WOLGAS95 predicted shear stress

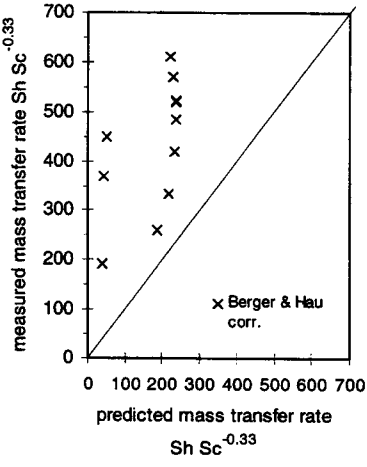

Figure 15. Comparison between measured and predicted mass transfer rates

- A comparison between the measured data and predictions with the steady state two/three phase flow code WOLGAS95 has been made. Predicted hold-up, pressure drop and mean wall shear stresses agreed reasonably well with the data.

- However, the mass transfer rate predictions based on WOLGAS95 and the Berger & Hau correlation gave large discrepancies compared to the measurements. Improved modelling of the mass transfer rates in multiphase flow thus seems to be necessary. In the literature the effects of bubbles on mass transfer rates have been reported and an improved modelling of these effects could turn out to be important. Another possibly important effect, which is not taken into account in the present mass transfer calculations, is the influence of waves at the interface.

ACKNOWLEDGEMENTS

The experiments described in this paper were carried out in a research project financed by Statoil a.s. Their support and permission to publish this paper is gratefully acknowledged. The authors also wish to thank Dag Thomassen for his help on the project.

REFERENCES

BELLHOUSE, B.J. and SCHULTZ, D.L., 'Determination of the mean and dynamic skin friction, separation and transition in low speed flow with a thin film heated element', Journal of Fluid Mech. 24, pp. 379 - 400 (1966)

BERGER, F.P. and HAU, K.F.F.L., 'Mass Transfer in Turbulent Pipe Flow Measured by the Electrochemical Method', Int. J. Heat and Mass Transfer, 1977, Vol. 20, pp. 1185 - 1194 (1977)

BROWN, G.L., 'Theory and Application of Heated Films for Skin Friction Measurement', Proceedings of the 1967 Heat Transfer and Fluid Mechanics Institute (Stanford U.P., Stanford California, 1967), pp. 361 -381, (1967)

CHEN, J.C., 'A Correlation for Boiling Heat Transfer to Saturated Fluid in Convective Flow', ASME-AICh Heat Transfer Conference and Exhibit, New York 17, N.Y.: The American Society of mechanical Engineers (ASME), 1963, paper no. 63-HT-34 (1963)

ECONOMOU, D. J. and ALKIRE, R. C., 'Two-Phase Mass Transfer in Channel Electrolysers with Gas-Liquid Flow', Journal of Electrochemical Society, 1985 March, Vol. 132 (no. 3), pp. 601-608 (1985)

GOWAN, HEWITT, OWEN and BURNETT, 'Wall Shear Stress Measurements in Vertical Air-water Annular Two-phase Flow', Int. J. Multiphase Flow Vol. 15, No. 3, pp 307 - 325 (1989)

KOWALSKI, J.E., 'Wall and Interfacial Shear Stress in Stratified Flow in a Horizontal Pipe', AIChE Journal, February 1987, Vol. 33, No. 2, pp. 274-281 (1987)

LUNDE, K., 'Gas entrainment into the liquid layer of stratified gas/liquid flow.', 6th Int. Symp. on Gas-Liquid Two-Phase Flows, 1997 ASME FED Summer Meeting, Vancouver, Br.C. (1997)

NYDAL, O.J., 'Liquid volume fraction measurements with a gamma densitometer and a conductance probe', 5'th Conf. on Multiphase Production, Cannes, June 1991, (1991)

NAKARYAKOV, V.E., KASHINSKY, O.N., KOZMENKU, B.K., 'Electrochemical Methods for Measuring Turbulent Characteristics of Gas-Liquid Flows', Symposium on Measuring Techniques in Gas-Liquid Two-Phase Flows, Nancy, France July 1983 (1983)

SHIRALKAR, B., 'A Study of the Liquid Film in Adiabatic Air-water Flow With and Without Obstacles', General Electric Report GEAP-10248 (1970)